HHS Public Access

Author manuscript

Sci Immunol. Author manuscript; available in PMC 2018 December 18.

Published in final edited form as:

Sci Immunol. 2018 August 17; 3(26): . doi:10.1126/sciimmunol.aat7796.

Antigen-specific antibody Fc-glycosylation enhances humoral immunity via the recruitment of complement

G Lofano[1], **MJ Gorman**[1], **AS Yousif**[1,2], **WH Yu**[1,3], **JM Fox**[4], **AS Dugast**[1], **ME Ackerman**[5], **TJ Suscovich**[1], **J Weiner**[5], **D Barouch**[1,6], **H Streeck**[7], **S Little**[8], **D Smith**[8,9], **D Richman**[8,9], **D Lauffenburger**[3], **BD Walker**[1,10,11], **MS Diamond**[4], and **G Alter**[12]

[1]Ragon Institute of MGH, MIT and Harvard, Cambridge, MA 02139, USA.

[2]Department of Immunology and Biotechnology, Tropical Medicine Research Institute, Khartoum, Sudan.

[3]Department of Biological Engineering, Massachusetts Institute of Technology, Cambridge, MA 02142, USA.

[4]Departments of Medicine, Molecular Microbiology, and Pathology & Immunology, Washington University School of Medicine, St. Louis, MO 63110, USA.

[5]Thayer School of Engineering, Dartmouth College, Hanover, NH 03755, USA.

[6]Center for Virology and Vaccine Research, Beth Israel Deaconess Medical Center, Boston, MA 02115, USA.

[7]Institut für HIV Forschung, Universität Duisburg-Essen, Essen, Germany.

[8]University of California, San Diego, San Diego, CA 92093, USA.

[9]VA San Diego Healthcare System, San Diego, CA 92161, USA.

[10]Institute for Medical Engineering and Science, Massachusetts Institute of Technology, Cambridge, MA 02139, USA.

[11]Howard Hughes Medical Institute, Chevy Chase, MD 20815, USA.

[12]Ragon Institute of MGH, MIT and Harvard, Cambridge, MA 02139, USA. galter@partners.org.

Abstract

HIV-specific broadly neutralizing antibodies (bNAbs) confer protection following passive immunization, but the immunological mechanisms that drive their development following HIV infection are poorly understood. Structural features of bNAbs indicate that they originate from extensive germinal center selection, which relies on persistent germinal center activity. However, why a fraction of infected individuals are able to successfully drive more effective affinity maturation is unclear. Delivery of antigens in the form of antibody-immune complexes (IC), that bind to complement receptors (CRs) or Fc-receptors (FcRs) on follicular dendritic cells (FDCs), represents an effective mechanism for antigen delivery to the GC. Thus we sought to define whether IC-FcR or CR interactions differ among subjects who develop broadly neutralizing antibody responses to HIV. Enhanced Fc-effector functions and FcR/CR interactions, via altered Fc-glycosylation profiles, were observed among subjects with neutralizing antibody responses to HIV compared to subjects without neutralizing antibody activity. Moreover, both polyclonal

Neutralizer ICs and monoclonal-IC mimics of Neutralizer antibodies induced higher antibody titers, higher-avidity antibodies, and expanded germinal center B cell reactions following immunization of mice, via accelerated antigen deposition within B cell follicles in a complement dependent manner. Thus, these data point to a direct role for altered Fc-profile/complement interactions in shaping the maturation of the humoral immune response, providing insights on how GC activity may be enhanced to drive affinity maturation in next generation vaccine approaches.

INTRODUCTION

The development of a protective vaccine against HIV will likely require the induction of highly cross-reactive, broadly neutralizing antibodies (bNAbs). While current vaccination regimens can readily induce antibodies capable of neutralizing autologous viruses(1, 2), these immunization strategies have generated only weakly cross-neutralizing (heterologous) antibodies(3, 4). Although vaccination has failed to induce antibodies with appreciable neutralization breadth, 5–30% of infected individuals naturally develop bNAbs, albeit after several years of infection(5, 6) and one step behind the autologous virus(7). Thus, elucidating the immunological processes that allow some individuals to overcome the immunologic barrier to developing neutralizing breadth may provide critical insights for the development of a vaccine capable of inducing bNAbs.

While our understanding of the molecular and structural features of antibodies that allow for broad neutralization has increased dramatically over the last decade(8, 9), the underlying immunological pathways that lead to these unusual features have yet to be fully elucidated. Nearly all bNAbs develop following extensive somatic hypermutation and often contain mutated framework regions(9, 10), features that are indicative of the prolonged affinity maturation. Importantly, previous studies have linked high viral loads, low CD4 T cell counts, and immune activation in the evolution of bNAbs(11–14). In the setting of low levels of viremia and high CD4 counts, bNAb activity still evolves, but only in the setting of a unique plasma type 1 interferon and GC-centric cytokine signature, pointing to the need for persistent GC activity(15). Yet, how these individuals maintain GC activity, particularly in the setting of low antigenic loads, is unclear.

Antigen delivery to the lymph node, and specifically to follicular dendritic cells (FDCs), plays a key role in both initiating and sustained the GC reaction(16). Specifically, antigen may be delivered to the lymph node via both “naked” antigen diffusion from the lymph or active antigen delivery via the delivery of antigen in the form of immune complexes (ICs) by non-cognate B cells or local macrophages(17–20). While HIV antigens likely arrive in the GC in the absence of Ab opsonization in acute HIV infection, high titers of HIV-specific antibodies (Abs) are induced over the course of infection that contribute to IC formation(21, 22), antigen capture and delivery, and seeding of antigens in the GC(23). However, whether differences in IC quality could contribute to GC generation and persistence, affinity maturation, and the evolution of neutralization breadth is unknown.

IC activity is modulated by both the Fab and Fc domains of the antibody. The Fab drives antigen specificity, whereas the Fc determines which innate immune receptors, including Fc receptors (FcRs) and complement receptors (CRs), ICs can bind. Depending on the FcRs

and CRs engaged by an IC, antigens can be rapidly destroyed or transported to the GC for antigen presentation(18, 19, 24–27). As such, modifications to the Fc domain, including changes in antibody isotype/subclass and antibody glycosylation(28–31), may have a profound impact on altering IC delivery, via improved IC affinity for particular FcRs/CRs. Along these lines, influenza-specific Fc antibody glycosylation post-vaccination is associated with enhanced affinity maturation of the influenza-specific response(32), highlighting the potential influence of the Fc-domain changes following vaccination with the antiviral activity of the vaccine induced immune response.

We thus speculated that qualitative changes in the Fc domain track with the development of bNAbs during HIV infection and point to the mechanism by which the Fc domain of the antibody may be leveraged to drive the evolution of highly affinity matured broadly neutralizing antibody responses. Using “Systems Serology”(33), significant differences in the Fc-profiles of HIV-specific antibodies were observed in individuals who developed neutralizing breadth (Neutralizers) compared to those who did not (Non-Neutralizers). Moreover, immunization with ICs generated with polyclonal antibodies from Neutralizers induced higher HIV-specific antibody responses post-vaccination. Importantly, this biological activity was linked to particular antibody glycosylation profiles, that when replicated with monoclonal IC immunization, resulted in enhanced IC capture by non-cognate B cells, accelerated IC deposition within B cell follicles, and elevated antibody titers and avidity antibody production in a complement dependent manner. Collectively, these data point to Fc-glycosylation as a direct modulator of B cell immunity, pointing to a novel avenue by which next generation vaccines may exploit both ends of the antibody to drive enhanced B cell affinity maturation that may be required against highly mutable targets.

RESULTS

Selective Fc functional profile differences exist among Neutralizers

Given previous associations of the evolution of neutralizing antibody breadth in the setting of high immune activation, low CD4 counts, and high viral loads(12, 14), we aimed to dissect the potential involvement of changes in immune complex (IC) biology in a group of spontaneous controllers of HIV (≤2000 copies/ml), a fraction of whom developed broad neutralizing antibody responses, despite the absence of high levels of plasma antigenemia(15). Seventy-one participants who were able to neutralize greater than 45% of tier 2 viruses (Neutralizers; N) was compared to a matched group of 60 participants with no evidence of neutralizing antibody breadth (0% neutralizing activity across 11 tier 2 viruses; Non-Neutralizers; NN). The two groups were matched for duration of infection, viral loads, and CD4 counts.

No differences in the ability of antibodies to recruit NK cells to kill HIV envelope–coated target cells in an antibody-dependent cellular cytotoxicity (ADCC) assay were observed between the Neutralizers and Non-Neutralizers (Figure 1A). In contrast, significant differences were observed in the capacity of Neutralizer antibodies to direct antibody-dependent cellular phagocytosis (ADCP) and antibody-dependent complement deposition (ADCD) (Figures 1B and C). Given the use of different Fc receptors used to drive these

innate functions, these data suggested that Neutralizer antibodies were selectively skewed to drive enhanced phagocytic and complement-depositing activity, but not NK cell cytotoxicity.

To further dissect the specific Fc receptors that were selectively recruited by Neutralizer antibodies, a multiparametric luminex assay was used to measure differences in IC binding to a spectrum of Fcγ receptors and complement proteins. Using a panel of HIV envelope-conjugated luminex beads, ICs were formed, and binding to the ICs by Fcγ receptors and complement was measured. Striking differences were observed among the Neutralizer and Non-Neutralizer antibodies in their ability to bind to both C1q and FcγRs (Figure 2). Enhanced binding to FcγR2B, FcγR3A and Fcγ3B, was observed in Neutralizer antibodies, with even more pronounced binding to FcγR2A and C1q (Fig. 2B). These data argue for an overall enhanced Fcγ receptor binding profile in antibodies from Neutralizers compared to Non-Neutralizers; however, this binding activity was more profoundly skewed towards FcγR2 and C1q binding. Moreover, longitudinal analysis of plasma samples from acutely infected individuals, half of whom went on to generate neutralizing antibodies, point to selectively elevated gp120-specific FcγR2 binding preceding to the evolution of bNAbs (Figure 2C). Given the importance of both FcγR2 and C1q in the delivery of IC cargo to the GC(17, 34, 35), these data point to unique IC profiles among Neutralizers with a higher intrinsic capacity to interact with Fc-binding proteins involved in antigen delivery to the GC, thereby potentially contributing to persistent GC activity and enhanced affinity maturation.

HIV-specific antibodies from Neutralizers promote germinal center reactions

To test the hypothesis that differences in Fc-profiles generated in Neutralizers and Non-Neutralizers were responsible for differences in GC reactions and affinity maturation, we generated ICs from Neutralizers and Non-Neutralizers. Specifically, recombinant HIV gp120 proteins were complexed with polyclonal antibodies from Neutralizers and Non-Neutralizers, and equivalent amounts of alum-adjuvanted ICs, alum-adjuvanted gp120, or alum alone were administered to mice. Mice received two immunizations, three weeks apart, and 10 days after the last immunization, gp120-specific antibody serum titers, high-avidity gp120-specific antibody titers, and the frequency of germinal center B cells in the draining lymph nodes of immunized mice were measured. As expected, higher levels of gp120-specific antibodies were induced in IC-immunized compared with mice vaccinated with antigen alone (Figure 3A). Mice immunized with the ICs from Neutralizers demonstrated slightly higher levels of overall antibody titers, as well as more avid antibodies compared to the mice vaccinated with ICs from Non-Neutralizers ($p<0.05$; Figure 3A–B). Furthermore, higher frequencies of germinal center ($CD19^{+}CD30^{-}CD95^{+}$) B cells were observed following immunization with ICs from Neutralizers compared to mice immunized with ICs from Non-Neutralizers (Figure 3C). These data suggest that the Fc-differences in Neutralizer antibodies may not only represent a biomarker of a more effective humoral immune response, but may directly contribute to differences in GC activity.

Unique antigen-specific antibody glycosylation and elevated IgG1 are enriched among Neutralizers

To specifically define the biophysical differences in Neutralizers and Non-Neutralizers IC profiles that may have contributed to enhanced humoral immune responses, differences in

both subclass selection levels and Fc-glycosylation profiles were interrogated on HIV-specific antibodies. While no differences were observed in antigen-specific IgG2, IgG3, and IgG4 levels across the two groups, Neutralizers possessed higher HIV-specific IgG1 titers to all HIV antigens, but not to influenza HA (Fig.4 A, B; Suppl.Fig.1), highlighting the infection-specific change in antibody levels. Thus, differences in IC activity may be attributable to higher overall HIV-specific IgG1 levels, which could account for improved overall FcR binding; however, selectively enhanced binding to C1q and FcγRII could not be explained by differential subclass selection differences.

Given the emerging appreciation for the role of antigen-specific antibody glycosylation in shaping Fc-activity(28, 29), we next profiled HIV-specific antibody glycosylation(36). Elevated levels of sialylated glycan structures were observed in HIV envelope specific IgGs from Neutralizers compared to Non-Neutralizers. In contrast, Non-Neutralizers possessed significantly higher levels of singly-galactosylated (G1) structures on their HIV-specific IgG1 antibodies (Figure 4C–D). Thus, selective differences in sialylation and galactosylation were observed among Neutralizers and Non-Neutralizers, pointing to qualitative differences in IgG1 antibody post-translational modifications across the two HIV infected groups.

To further define the minimal HIV-specific features that were selectively enriched among Neutralizers, an orthogonal multivariate partial least square discriminant analysis (PLSDA) was used, combining all gp120-specific features. Using Fc-profiles features alone, nearly complete separation was observed between Neutralizers and Non-Neutralizers (Figure 4E). The dominant features that selectively split the 2 groups, included the level of sialylated glycan structures and overall levels of gp120-specific IgG1 antibodies, with the percentage of sialylated gp120-specific antibodies ranking as the top feature required to separate the two groups (Fig.4 E–F). In line with previous studies pointing to an association between the levels of vaccine-induced sialylated antibodies and antibody affinity maturation(32), sialylated HIV-specific antibodies were selectively enriched among Neutralizers, pointing to a potentially critical link between post-translational antibody sialylation and affinity maturation across disease and vaccination. However, whether sialylation represents a simple biomarker of a more highly affinity matured immune response or whether it directly contributes to affinity maturation is largely unknown.

HIV antibody glycoforms modulate IC-driven innate and adaptive immunity

To specifically define the direct involvement of sialylated antibodies in driving affinity maturation, we immunized animals with ICs generated with a single Fab domain, but with differential glycosylation. ICs were generated with an HIV-specific monoclonal antibody (PGT121) that was fractionated and enzymatically prepared into three separate antibody Fc-fractions to generate: agalactosylated ICs (G0-ICs), non-sialylated galactosylated ICs (G1/G2 NS-ICs), or sialylated ICs (G1/G2 S-ICs). Importantly, no differences were observed in fraction-affinity by ELISA (Supplemental Figure 2). Again, mice were immunized with alum formulated ICs, alum-formulated antigen alone, or alum alone, and antibody levels, avidity, and B cell frequencies were interrogated 10 days after the second immunization. Strikingly, mice immunized with the S-ICs exhibited both increased gp120-specific IgG titers compared to mice immunized with NS-ICs, G0-ICs, or gp120 alone

(Figure 5A). Moreover, immunization with S-ICs also drove more avid gp120-specific antibodies compared all other immunized groups (Figure 5A). These data implicate Fc sialylation as a direct modulator of the humoral immune response, rather than a simple biomarker of a more highly affinity matured response.

Sialylated ICs drive enhanced antigen deposition

To begin to dissect the mechanism by which S-ICs may contribute to enhanced B cell affinity maturation, we examined the distribution of these ICs early following immunization. A number of cells have been implicated in IC capture and transfer to GCs, including sinusoidal macrophages (SSM)s and non-cognate B cells that collectively are involved in transferring ICs to FDCs. Glycan-fractionated PGT121-ICs were therefore prepared with a fluorescently labeled-gp120. The ICs were delivered intravenously and IC capture was measured by flow cytometry and immunofluorescent microscopy 1 and 3 hours following IC administration. After 1 hour, significantly higher frequencies of ICs were observed on B cells and FDCs in the presence of S-ICs compared to NS-ICs or antigen alone (Figure 5B); after 3 hours, SSMs, B cells, and FDCs captured significantly higher levels of ICs in the presence of sialylated antibodies.

To further visualize the localization of the ICs after delivery, fluorescence microscopy was performed on splenic follicles. One hour after vaccination, follicles from mice that received the sialylated ICs exhibited greater IC deposition within the follicle compared to mice that received the non-sialylated ICs (Figure 5C). Moreover, S-IC deposition appeared to be located close to FDCs, whereas NS-IC deposition, though infrequent, was largely observed in closer proximity to SSMs. Furthermore, vaccination with the sialylated ICs induced a higher number of gp120-positive FDC areas per follicle, two on average, and of larger size, compared to vaccination with non-sialylated ICs (Figure 5D). Furthermore, after 3 hours, greater antigen-deposition was observed in the presence of the S-ICs compared to the NS-ICs, co-localizing with germinal center B cells (GL-7) (Figure 5E). These data therefore suggest that S-ICs may contribute to enhanced humoral immune activity via the rapid and effective deposition of ICs within GCs via enhanced IC capture and delivery to the follicle. However, how these sialylated ICs may be selectively captured and delivered to the follicle is unknown.

Sialylated Fc antigen effects are complement dependent

Emerging data suggest that complement plays an essential role in IC mediated antigen deposition on FDCs(17). Thus, we next aimed to determine whether uptake of sialylated ICs depends on complement. Using a non-cognate reporter B cell line, Raji cells, expressing both complement receptors and Fc receptors(37–39) we assessed the capture S-ICs, NS-ICs in the presence or absence of complement and/or anti-FcγR2B by flow cytometry. As expected, at the highest concentrations, both S- and NS-ICs were trapped by the non-cognate B cells in the presence of complement; however, S-ICs were able to bind at higher levels in the presence of complement compared to NS-ICs. In contrast, no difference was observed between S- and NS-ICs in the setting of FcγR2B blockade (Figure 5F). These data argue for a dominant role for S-IC interaction with complement in IC capture.

To confirm the interaction between S-ICs and complement, we next performed IC-based immunization in complement-deficient mice. Wild type or *C1q*-deficient mice were immunized twice with the ICs or antigen alone. As expected, antigen-specific antibody responses were highest in the wild type mice immunized with S-ICs, with intermediate levels observed in wild type mice vaccinated with NS-ICs or antigen alone (Figure 5G). However, a significant reduction in antibody titers and avidity were observed in the *C1q*-deficient mice vaccinated with S-ICs compared to wild-type mice (Figure 5G). Moreover, while all animals appeared to reach a plateau following the second boost, the C1q-knockout mice immunized with S-ICs exhibited significantly lower titers and lower avidity antibody induction compared to their wild type counterparts (Figure 5G). These data provide further evidence to support a role in antibody sialylation in complement-dependent IC delivery for B cell priming and boosting. While these data do not preclude a role for other Fc receptors in IC-mediated antigen deposition in the lymph node, they strongly support a critical role for sialylated antibody–induced complement deposition as a driver of high-affinity B cell responses.

DISCUSSION

While efforts towards vaccine design to induce broadly neutralizing antibodies have resulted in limited success in driving weak tier 2 heterologous immunity, understanding the immunological features that allow some individuals to develop broad cross-tier neutralizing breadth may accelerate the path to the induction of these unusual, but protective, responses. Here, we observed that individuals who developed bNAbs possessed HIV-specific antibodies with enhanced CR and FcγR binding, selectively skewed to induce phagocytosis and complement deposition, via enhanced HIV-specific antibody Fc-domain sialylation. Given the importance of Fc binding for antigen deposition in the GC and our emerging appreciation for enhanced and persistent GC activation among individuals with neutralizing antibodies(10, 12, 15, 40), we speculated that the enhanced Fc functionality could actively contribute to the evolution of HIV-specific neutralization breadth. Remarkably, ICs generated with either antibodies from individuals with these enhanced Fc functions or with highly sialylated monoclonal antibodies induced both higher antibody titers and more avid antibodies following IC immunization. Thus, these data suggest that the Fc domain of the antibody may play a critical role in the formation of the GC reaction, catalyzing the persistent selection and affinity maturation of B cells that may be required to drive the unusual B cell selection associated with the development of bNAbs against HIV.

Rational vaccine design has led to the creation of both stabilized trimers and minimal scaffolds able to focus the immune response to sites of neutralization vulnerability(8, 41, 42). However, vaccination with these constructs continue to induce antibodies with narrow breadth, likely due to the limited amount of affinity maturation that is observed following immunization. This has led the field to explore novel immunization strategies and alternate adjuvants, as well as to focus vaccine design on the elicitation of bNAbs able to drive broad neutralization in the absence of high levels of somatic hypermutation(6, 43, 44). The data presented here suggest that naturally modified antibodies can selectively augment the level of affinity maturation via the rapid capture and delivery of antigens to the GC. First observed in the context of influenza vaccination, the level of influenza hemagglutinin-specific

antibody sialylation was associated with the level of affinity maturation(32). Here, the administration of selectively glycosylated antibodies at the time of antigen exposure led to a dramatic increase in antigen deposition and maturation of high avidity antibodies, pointing to a direct role for antigen-specific antibody glycosylation as a direct contributor to GC activity. Moreover, mounting data suggest that antibody glycosylation is programmed in an antigen-specific manner(45), is modulated by vaccination(45, 46), and is tuned by adjuvants(47), offering a potential opportunity to strategically manipulate the quality of antibodies following a prime, to enhance immunity upon boosting.

Beyond the role of immune activation, low CD4 T cell counts, and high viral loads as drivers of neutralizing antibody breadth, recent data suggest that individuals who generate bNAbs possess autoimmune-like transcriptional signatures(48–50). These autoimmune like signatures may enable B cells to break the necessary tolerance to select B cells that target HIV-envelope epitopes that cross-react with self-like antigens as well as to drive extraordinary affinity maturation(5, 50, 51), even within frame-work regions that are rarely targeted for somatic mutation in healthy B cells(10). Similarly, IC levels and signaling have been linked to autoimmune signatures in B cells in subjects with rheumatoid arthritis and lupus(52–54). However, whether Neutralizers possess autoimmune-like signatures due to intrinsic differences in their B cell populations or due to the higher abundance of ICs able to interact with FcRs and CRs is unknown. Nevertheless, it is plausible that increased IC signaling could not only lead to enhanced antigen deposition, but to increasing B cell activation, enabling antigen-specific B cells to undergo more extensive maturation, tolerate more mutations, and even develop responses to cross-reactive epitopes. Thus, linked to emerging rationally designed antigens, immunization strategies that also selectively direct the Fc domain of the induced humoral immune response may stimulate the needed activation and maturation to induce protective immunity driven by sophisticated new immunogens.

Complement has been shown to play a vital role in IC delivery to FDCs(17, 19, 20); however, the specific antibody modifications that enable more effective IC capture within GCs has been less clear. A number of different cells contribute to the delivery of ICs to the GC including naïve non-cognate B cells and macrophages, which typically acquire ICs via different combinations of FcRs and CRs(34, 55, 56). However, previous associations between sialylated HA-specific antibodies and affinity maturation(32) have suggested that enhanced IC deposition was linked to CD23 (FcεRII), which is highly expressed on B cells. While CD23 may play a role in affinity maturation(57), the data presented here build on our previous understanding of the critical role of complement in IC capture and deposition on FDCs and provide evidence for a mechanistic involvement of sialylation in the acceleration of antigen deposition and B cell maturation. Whether the deposited ICs accelerate affinity maturation by simply providing more antigen to drive higher frequencies of B cells that must compete more aggressively for limited T cell help or lead to tighter binding ICs that require B cell receptors to capture antigen more “avidly” for survival signals is unclear. However, the data clearly highlight the “adjuvanting” activity of sialylated antibodies in B cell maturation, pointing to potential new opportunities to leverage the Fc domain to drive enhanced affinity maturation in the context of HIV vaccination.

Complement-activating antibodies have also been implicated in the destruction of HIV virions(58). Thus, sialylation may provide a bifunctional advantage in simultaneously driving enhanced affinity maturation as well as direct antiviral control of HIV. Thus, while HIV can rapidly mutate to escape the selection pressure from neutralizing antibodies in the context of natural infection, it is plausible that vaccines able to induce complement-depositing antibodies against HIV may enhance both Fab- and Fc-mediated control of the virus upon exposure. Thus, with our emerging understanding of the opportunities to directly program antibody glycosylation, via distinct immunogens(45) or adjuvants(47), next-generation vaccine strategies may now harness the full antiviral breadth of the humoral immune response. Therefore, coupled to sophisticated emerging immunogens, manipulation of the Fc domain of the antibody may support the evolution of neutralizing antibodies aimed at blocking HIV infection.

MATERIALS and METHODS

Study subjects

A total of 131 controllers were included for cross-sectional studies, including both elite controllers (ECs), who spontaneously control viral replication to undetectable levels (<75 copies/mL, CD4:353–1813 cells/mm3) and viremic controllers (VCs) with detectable but low viral loads (~20–1658 copies of RNA/mL and CD4:172–1794 cells/mm^3)(15). All subjects signed informed consent and the study was approved by the MGH institutional review board. HIV-1 neutralization breadth was assessed using the TZM-bL cell–based pseudovirus neutralization assay, as described in(59) against a panel of Env-pseudoviruses derived from nine Clade B Tier 2 and two Tier 3 neutralization sensitivities: AC10.0.29, RHPA4259.7, THRO4156.18, REJO4541.67, WITO4160.33, TRO.11, SC422661.8, QH0692.42, CAAN5342.A2 and Tier 3: PVO.4 and TRJO4551.58. Neutralization was defined as at least 50% inhibition of infection at a 1:20 dilution. The neutralization breadth was defined as the percentage of the 11 isolates neutralized by each plasma sample; Neutralizers had more than 20% cross-neutralizing activity, Non-Neutralizers had undetectable cross-neutralization against tier 2/3 viruses. All samples that showed reactivity to the murine leukemia virus–pseudotyped virion controls were excluded.

Additionally, longitudinal plasma samples were included from 26 acutely infected individuals who were recruited as part of the San Diego Acute and Early Infectious Disease Research Program(7). Twelve individuals developed neutralizing antibody breadth following 2–3 years of infection, whereas 14 individuals (matched for age, gender, and ethnicity) did not develop any appreciable tier 2 neutralizing antibody breadth. Plasma samples were analyzed at 1month, 6months, and 1year post-estimated time of infection. These limited time-points were included to ensure that sampling occurred prior to the evolution of neutralizing antibody breadth, but to maintain consistency in comparison for matched durations of infection.

All subjects provided informed consent at their respective institutions.

Functional assays

Antibody-dependent cellular phagocytosis (ADCP) assay: The THP-1 phagocytosis assay was performed as previously described(60). Briefly, THP-1 cells were purchased from ATCC and cultured as recommended. Biotinylated rgp120-YU2 (Immune Technology) was used to saturate the binding sites on 1 μm fluorescent neutravidin beads (Invitrogen) overnight at 4°C. Excess antigen was removed by washing, and then beads were incubated with patient antibody samples for 2hr at 37°C. Following opsonization, THP-1 cells were added, and were incubated overnight to allow phagocytosis. The cells were then fixed, and the extent of phagocytosis was measured via flow cytometry on a BD LSR II flow cytometer equipped with high-throughput sampler. The data are reported as a phagocytic score, which takes into account the proportion of effector cells that phagocytosed and the degree of phagocytosis (integrated MFI: frequency × MFI). Each antibody sample was tested over a range of concentrations (0.1–100 μg/ml).

Antibody-dependent cellular cytotoxicity (ADCC) assay: The rapid fluorescent ADCC (RFADCC) assay was performed as previously described(61). In brief, CEM-NKr cells were pulsed with rgp120-YU2 proteins (6 μg/ml) and labeled with the intracellular dye CFSE and the membrane dye PKH26. NK cells were enriched directly from seronegative donor whole blood by negative selection using RosetteSep (Stem Cell Technologies). Purified IgG was added to the labeled, antigen-pulsed CEM-NKr cells prior to the addition of fresh NK cells. The cells were incubated for 4 hr at 37°C and then fixed. The proportion of cells that maintained membrane expression of PKH26 but lost CFSE staining (i.e., lysed cells) were quantified via flow cytometry.

Antibody-dependent complement deposition (ADCD): Ab-dependent complement deposition was assessed by the measurement of complement component C3b on the surface of target cells. CD4-expressing target cells were pulsed with the rgp120-YU2 protein, and incubated with serum antibodies. Freshly isolated HIV negative donor plasma diluted into veronal buffer with 0.1% gelatin (1:10 dilution) and the cells were incubated for 20 min at 37°C. The cells were then washed with 15 mM EDTA in PBS, and complement deposition was detected via flow cytometry following staining for C3b (Cedarlane). Replicates using heat inactivated donor plasma were used as negative controls.

ICs uptake by Raji B cells: biotinylated avitag-gp120-YU2 (ImmuneTech) was combined with APC-labeled streptavidin (Invitrogen) for 2h at 37°C. Serial dilutions of Sialylated-PGT121 or Non-Sialylated-PGT121 antibodies were added to prepare the S-ICs or NS-ICs respectively. Then, immune complexes were washed with PBS+5% BSA and incubated with 50,000 Raji B cells/well for 30 minutes at 37˚C with or without freshly isolated serum from a human healthy donor in presence or absence of anti-FcγR2B antibody. Cells were fixed with 100uL PFA 4% and the percentage of ICs^+ Raji B cells was measured by flow cytometry.

Luminex Subclass Assay, FcγR and Complement proteins binding

A custome Luminex assay was used to quantify the relative concentration of HIV-specific antibody subclass levels among the HIV-specific antibodies as previously described(62).

Briefly, microplex carboxlyated beads (Luminex) were coupled to the indicated proteins via covalent NHS-ester linkages by combining EDC and NHS (Thermo Scientific) in PBS, as recommending by the manufacturer (antigens: gp140-SF162, gp120-YU2, gp41-HXBc2, p24-HXBc2, HA-Brisbane/60/09). The coupled beads (50μl of a 100 microspheres/μl solution in 0.1% BSA in PBS) were added to each well of a 96-well filter plate (Millipore). The purified IgGs (50μl of each sample diluted to 200 μg IgG/ml) were added to five wells of the 96-well plate and incubated at 4°C overnight. The beads were washed three times with 100μl of PBS-Tween, and individual IgG isotype detection reagents (bulk IgG, IgG1, IgG2, IgG3, and IgG4) conjugated to PE (Southern Biotech) were added individually to each of one of the five wells. The 96-well plate was incubated with shaking for 2 hr, washed three times, and read on Bio-Plex 200. Similarly, FcγIIA, FcγIIB, FcγIIIA, FcγIIIB and C1q were conjugated to PE (Southern Biotech) and used to test the Fc-receptors and complement proteins binding capacity of HIV-specific antibodies.

Glycan analysis

The relative abundance of antibody glycan structures was quantified by capillary electrophoresis, as previously described(36). Briefly, antigen-specific antibodies were purified using gp120-coupled magnetic beads (New England BioLabs), then treated with IdeZ protease (New England BioLabs) to collect the antibody Fc portion. N-glycans were removed from the Fc domains and labeled with APTS using the GlycanAssure™ APTS Kit (Thermo Fisher) as described in the manufacturer's protocol. Labeled glycans were loaded onto a 3500 Genetic Analyzer (Thermo Fisher). Peaks of 5 major glycan structures (G0, G1, G2, Bisecting and Sialylated) were identified, and the relative abundance of each structure was determined by calculating the area under the curve of each peak divided by the total area of all peaks.

Purification of antibody glycoforms and immune complexes

PGT121 mAb was used to generate agalactosylated, galactosylated non-sialylated and galactosylated sialylated antibodies and then formulated with gp120 to prepare G0-ICs, NS-ICs and S-ICs respectively. Sialylated PGT121 mAb was used to generate non-sialylated and agalactosylated antibodies. The antibody was incubated overnight at 37°C with Neuraminidase (Millipore Sigma) or Galactosidase S (New England BioLabs) to generate non-sialylated or agalactosylated antibodies respectively. Glycoprofiles of the modified mAbs was confirmed by glycan sequencing and by western blot using SNA-biotin that binds to sialic acid. Fc glycoform composition without neuraminidase treatment was 13,14% sialylated (G2S1F), 86.86% neutral (G0F, G1F, G1FB, G2F); Sialylated or Galactosylated glycoforms were not detected following neuraminidase or Galactosidase S treatment, respectively. Neuraminidase-treated non-sialylated PGT121 retained its ability to bind efficiently to gp120 (Suppl.Fig.2). For the preparation of immune complexes, biotinylated avitag-gp120-YU2 (ImmuneTech) was combined with APC-labeled or unlabeled streptavidin (Invitrogen) for 2h at 37°C. G0-PGT121, S-PGT121 or NS-PGT121 antibodies were added at a ratio of 1:2 antigen:antibody and incubated overnight at 4°C. Immune complexes generated from pooled sera from Neutralizers or Non-Neutralizers were prepared by using streptavidin-coupled beads, with a ratio 1:30 antigen:total IgGs; excess antigen and antibodies were removed by washing the pelleted beads.

Mice and vaccinations

Pathogen-free BALB/c female mice (Jackson Laboratories) aged 6 weeks were used in this study. All animal studies were carried out in compliance with current regulations of the MGH Center for Comparative Medicine at the Ragon Institute animal facility. To measure the frequencies of gp120+ immune cells by flow cytometry and detect the B cell follicles by confocal microscopy, mice received one intravenous vaccination with fluorescently labeled ICs in PBS. In order to measure the gp120-specific antibody and B cell responses, mice received two intramuscular vaccinations with alum-adjuvanted ICs three weeks apart, and then analysis was performed 10 days after last immunization. All formulations were adjusted with PBS to bring up to 100ul/mouse. C1q knockout mice in a C57BL/6 background and C57BL/6 wild type mice were used to assess the role of the C1q complement protein following vaccination; C57BL/6 mouse experiments were approved and performed according to the guidelines of the Washington University School of Medicine Animal Safety Committee. Immune complexes were prepared as described above.

Flow cytometry

For the characterization of the innate and the germinal center B cell responses, cell suspensions prepared from spleen, or pairs of draining inguinal lymph nodes from each mouse, were stained with blue live/dead cell stain (Invitrogen) for 20 min at room temperature and then incubated with Fc block (BD Biosciences) in PBS plus 1% FBS (HyClone, Thermo Scientific) for 10 min at 4˚C. Approximately 10^7 splenocytes or 2–3×10^6 lymph node cells were stained for 30 min at 4˚C with the following mAbs: anti-CD19 APC-H7 (BD Biosciences), anti-CD3 BV785 (BioLegend), anti-CD38 PerCP-C5.5 (BD Biosciences), anti–CD95 BV510 (BD Horizon). Cells were analyzed on a FACS Fortessa (BD Biosciences) and data analyses were performed using FlowJo software v9.6 (Tree Star).

Mouse antibody titers and avidity measurement

Titration of gp120-specific serum IgG was performed on individual serum samples with ELISA plates (Nunc MaxiSorp, Thermo Scientific) coated overnight with gp120-YU2 (250ng/ml). Plates were blocked with 2% BSA in PBS/Tween 20 0.05% for 1 h at 37˚C, and then washed three times with 0.05% Tween 20 in PBS and incubated for 2 h at 37˚C with individual mouse sera in 2-fold serial dilutions. Plates were washed, incubated for 1h at 37˚C with secondary anti-mouse total IgG (1:2000; Sigma-Aldrich), washed, and TMB was added for detection. The color reaction was measured with Tecan reader by determining the OD at 450nm, which was used to plot the graphs. Avidity was measured as the titer of high-avidity antibodies that were not washed away after plate washing with urea 7M for 15 min before the addition of the secondary antibody(63).

Confocal Microscopy

Spleens were collected from immunized animals at the appropriate time points, immediately frozen in OCT, and stored in liquid nitrogen until processing. The cryosections (8 mm thick) were cut along the entire organ to analyze all the planes of the organs. The cryosections were fixed using PBS plus 3% formaldehyde for 10 min at room temperature, washed twice with PBS, and stained using anti-CD35 (IgG purified, BD Pharmigen) or anti-GL-7 (IgM

purified, eBioscience) followed by rat anti-IgG Alexa568 (Abcam) or by rat anti-IgM TexasRed (Sigma) respectively. Sections were also stained with anti-CD169 (FITC, Biolegend); the antigen APC-labelled gp120 used for the immunizations was detected in the blue channel. After washing three times with PBS, stained tissue sections were sealed using Gold Antifade reagent (Invitrogen-Life Technologies) and a coverslip. Images were acquired with the Zeiss LSM 510 Confocal Microscope.

Statistical analysis

Partial least squares discriminant analysis (PLSDA) defined the relationship between the input as a linear combination of all features among Neutralizers or Non-Neutralizers(33). Specifically, PLSDA seeks the latent variables, which linearly combine all features, that explain the maxim variance between the groups; as result, this approach provides the generation of a model with the greatest separation among groups with the lowest possible mean squared error (MSE). Prior to PLSDA analysis, the data were normalized with mean centering and variance scaling; 10-fold cross-validation was performed by iteratively random exclusion of subsets of sample data (in groups of 10%) during model calibration, and then the excluded data were used to test model predictions. Ultimately, each variable identified in the model was weighted for its contribution to splitting the groups, aimed at generating a variable importance in projection (VIP).

ANOVA, followed by Tukey's or Bonferroni's post-tests, was performed using GraphPad Prism 7 software (GraphPad Software) to compare differences between more than 2 groups. T-tests were used to compare differences between groups using GraphPad Prism 7. Spider plots where generated with Microsoft Excel 2011.

Supplementary Material

Refer to Web version on PubMed Central for supplementary material.

ACKNOWLEDGEMENTS

This work was supported the National Institute of Health (R37AI080289 and R01AI102660), the Bill and Melinda Gates Foundation CAVD (OPP1066973), and the Ragon Institute of MGH, MIT and Harvard and the UCSD CFAR AI306214.

REFERENCES

1. Burton DR, Mascola JR, Antibody responses to envelope glycoproteins in HIV-1 infection. Nat Immunol 16, 571–576 (2015). [PubMed: 25988889]
2. Sanders RW et al., HIV-1 VACCINES. HIV-1 neutralizing antibodies induced by native-like envelope trimers. Science 349, aac4223 (2015). [PubMed: 26089353]
3. Pauthner M et al., Elicitation of Robust Tier 2 Neutralizing Antibody Responses in Nonhuman Primates by HIV Envelope Trimer Immunization Using Optimized Approaches. Immunity 46, 1073–1088 e1076 (2017). [PubMed: 28636956]
4. Zhou T et al., Multidonor analysis reveals structural elements, genetic determinants, and maturation pathway for HIV-1 neutralization by VRC01-class antibodies. Immunity 39, 245–258 (2013). [PubMed: 23911655]
5. Borrow P, Moody MA, Immunologic characteristics of HIV-infected individuals who make broadly neutralizing antibodies. Immunol Rev 275, 62–78 (2017). [PubMed: 28133804]

6. Mascola JR, Haynes BF, HIV-1 neutralizing antibodies: understanding nature's pathways. Immunol Rev 254, 225–244 (2013). [PubMed: 23772623]
7. Richman DD, Wrin T, Little SJ, Petropoulos CJ, Rapid evolution of the neutralizing antibody response to HIV type 1 infection. Proc Natl Acad Sci U S A 100, 4144–4149 (2003). [PubMed: 12644702]
8. Burton DR et al., A Blueprint for HIV Vaccine Discovery. Cell Host Microbe 12, 396–407 (2012). [PubMed: 23084910]
9. Irani V et al., Molecular properties of human IgG subclasses and their implications for designing therapeutic monoclonal antibodies against infectious diseases. Mol Immunol 67, 171–182 (2015). [PubMed: 25900877]
10. Klein F et al., Somatic mutations of the immunoglobulin framework are generally required for broad and potent HIV-1 neutralization. Cell 153, 126–138 (2013). [PubMed: 23540694]
11. Mikell I et al., Characteristics of the earliest cross-neutralizing antibody response to HIV-1. PLoS Pathog 7, e1001251 (2011). [PubMed: 21249232]
12. Sather DN et al., Factors associated with the development of cross-reactive neutralizing antibodies during human immunodeficiency virus type 1 infection. J Virol 83, 757–769 (2009). [PubMed: 18987148]
13. Cortez V, Odem-Davis K, McClelland RS, Jaoko W, Overbaugh J, HIV-1 superinfection in women broadens and strengthens the neutralizing antibody response. PLoS Pathog 8, e1002611 (2012). [PubMed: 22479183]
14. Gray ES et al., The neutralization breadth of HIV-1 develops incrementally over four years and is associated with CD4+ T cell decline and high viral load during acute infection. J Virol 85, 4828–4840 (2011). [PubMed: 21389135]
15. Dugast AS et al., Virus-driven Inflammation Is Associated With the Development of bNAbs in Spontaneous Controllers of HIV. Clin Infect Dis 64, 1098–1104 (2017). [PubMed: 28158448]
16. Allen CD, Okada T, Cyster JG, Germinal-center organization and cellular dynamics. Immunity 27, 190–202 (2007). [PubMed: 17723214]
17. Carroll MC, Isenman DE, Regulation of humoral immunity by complement. Immunity 37, 199–207 (2012). [PubMed: 22921118]
18. Gonzalez SF et al., Trafficking of B cell antigen in lymph nodes. Annu Rev Immunol 29, 215–233 (2011). [PubMed: 21219172]
19. Batista FD, Harwood NE, The who, how and where of antigen presentation to B cells. Nat Rev Immunol 9, 15–27 (2009). [PubMed: 19079135]
20. Phan TG, Green JA, Gray EE, Xu Y, Cyster JG, Immune complex relay by subcapsular sinus macrophages and noncognate B cells drives antibody affinity maturation. Nat Immunol 10, 786–793 (2009). [PubMed: 19503106]
21. Krapf FE, Herrmann M, Leitmann W, Schwartlander B, Kalden JR, Circulating immune complexes in HIV-infected persons. Klin Wochenschr 68, 299–305 (1990). [PubMed: 2139906]
22. Korolevskaya LB, Shmagel KV, Shmagel NG, Saidakova EV, Systemic activation of the immune system in HIV infection: The role of the immune complexes (hypothesis). Med Hypotheses 88, 53–56 (2016). [PubMed: 26880638]
23. Zeng M, Haase AT, Schacker TW, Lymphoid tissue structure and HIV-1 infection: life or death for T cells. Trends Immunol 33, 306–314 (2012). [PubMed: 22613276]
24. Bergtold A, Desai DD, Gavhane A, Clynes R, Cell surface recycling of internalized antigen permits dendritic cell priming of B cells. Immunity 23, 503–514 (2005). [PubMed: 16286018]
25. Gonzalez SF et al., Complement-dependent transport of antigen into B cell follicles. J Immunol 185, 2659–2664 (2010). [PubMed: 20724732]
26. Heesters BA et al., Endocytosis and recycling of immune complexes by follicular dendritic cells enhances B cell antigen binding and activation. Immunity 38, 1164–1175 (2013). [PubMed: 23770227]
27. Harwood NE, Batista FD, The antigen expressway: follicular conduits carry antigen to B cells. Immunity 30, 177–179 (2009). [PubMed: 19239901]

28. Jefferis R, Isotype and glycoform selection for antibody therapeutics. Arch Biochem Biophys 526, 159–166 (2012). [PubMed: 22465822]
29. Lux A, Yu X, Scanlan CN, Nimmerjahn F, Impact of immune complex size and glycosylation on IgG binding to human FcgammaRs. J Immunol 190, 4315–4323 (2013). [PubMed: 23509345]
30. Nimmerjahn F, Ravetch JV, Antibody-mediated modulation of immune responses. Immunol Rev 236, 265–275 (2010). [PubMed: 20636822]
31. Nimmerjahn F, Ravetch JV, Fcgamma receptors: old friends and new family members. Immunity 24, 19–28 (2006). [PubMed: 16413920]
32. Wang TT et al., Anti-HA Glycoforms Drive B Cell Affinity Selection and Determine Influenza Vaccine Efficacy. Cell 162, 160–169 (2015). [PubMed: 26140596]
33. Chung AW et al., Dissecting Polyclonal Vaccine-Induced Humoral Immunity against HIV Using Systems Serology. Cell 163, 988–998 (2015). [PubMed: 26544943]
34. Pincetic A et al., Type I and type II Fc receptors regulate innate and adaptive immunity. Nat Immunol 15, 707–716 (2014). [PubMed: 25045879]
35. Stokol T et al., C1q governs deposition of circulating immune complexes and leukocyte Fcgamma receptors mediate subsequent neutrophil recruitment. J Exp Med 200, 835–846 (2004). [PubMed: 15466618]
36. Mahan AE et al., A method for high-throughput, sensitive analysis of IgG Fc and Fab glycosylation by capillary electrophoresis. J Immunol Methods 417, 34–44 (2015). [PubMed: 25523925]
37. Theofilopoulos AN, Wilson CB, Dixon FJ, The Raji cell radioimmune assay for detecting immune complexes in human sera. J Clin Invest 57, 169–182 (1976). [PubMed: 128562]
38. Wang RY et al., Preferential association of hepatitis C virus with CD19(+) B cells is mediated by complement system. Hepatology 64, 1900–1910 (2016). [PubMed: 27641977]
39. Heesters BA et al., Follicular Dendritic Cells Retain Infectious HIV in Cycling Endosomes. PLoS Pathog 11, e1005285 (2015). [PubMed: 26623655]
40. Cohen KW, Dugast AS, Alter G, McElrath MJ, Stamatatos L, HIV-1 single-stranded RNA induces CXCL13 secretion in human monocytes via TLR7 activation and plasmacytoid dendritic cell-derived type I IFN. J Immunol 194, 2769–2775 (2015). [PubMed: 25667414]
41. Ofek G et al., Elicitation of structure-specific antibodies by epitope scaffolds. Proc Natl Acad Sci U S A 107, 17880–17887 (2010). [PubMed: 20876137]
42. Sanders RW, Moore JP, Native-like Env trimers as a platform for HIV-1 vaccine design. Immunol Rev 275, 161–182 (2017). [PubMed: 28133806]
43. Davenport TM et al., Somatic Hypermutation-Induced Changes in the Structure and Dynamics of HIV-1 Broadly Neutralizing Antibodies. Structure 24, 1346–1357 (2016). [PubMed: 27477385]
44. Francica JR et al., Analysis of immunoglobulin transcripts and hypermutation following SHIV(AD8) infection and protein-plus-adjuvant immunization. Nat Commun 6, 6565 (2015). [PubMed: 25858157]
45. Mahan AE et al., Antigen-Specific Antibody Glycosylation Is Regulated via Vaccination. PLoS Pathog 12, e1005456 (2016). [PubMed: 26982805]
46. Selman MH et al., Changes in antigen-specific IgG1 Fc N-glycosylation upon influenza and tetanus vaccination. Mol Cell Proteomics 11, M111 014563 (2012).
47. Francica JR et al., Innate transcriptional effects by adjuvants on the magnitude, quality, and durability of HIV envelope responses in NHPs. Blood Advances 1, 2329–2342 (2017). [PubMed: 29296883]
48. Bonsignori M et al., An autoreactive antibody from an SLE/HIV-1 individual broadly neutralizes HIV-1. J Clin Invest 124, 1835–1843 (2014). [PubMed: 24614107]
49. Euler Z et al., Cross-reactive neutralizing humoral immunity does not protect from HIV type 1 disease progression. J Infect Dis 201, 1045–1053 (2010). [PubMed: 20170371]
50. Moody MA et al., Immune perturbations in HIV-1-infected individuals who make broadly neutralizing antibodies. Sci Immunol 1, aag0851 (2016). [PubMed: 28783677]
51. Schroeder KMS et al., Breaching peripheral tolerance promotes the production of HIV-1-neutralizing antibodies. J Exp Med 214, 2283–2302 (2017). [PubMed: 28698284]

52. Clynes R, Immune complexes as therapy for autoimmunity. J Clin Invest 115, 25–27 (2005). [PubMed: 15630438]

53. Marrack P, Kappler J, Kotzin BL, Autoimmune disease: why and where it occurs. Nat Med 7, 899–905 (2001). [PubMed: 11479621]

54. Tsokos GC, Lo MS, Costa Reis P, Sullivan KE, New insights into the immunopathogenesis of systemic lupus erythematosus. Nat Rev Rheumatol 12, 716–730 (2016). [PubMed: 27872476]

55. Bournazos S, Ravetch JV, Fcgamma receptor pathways during active and passive immunization. Immunol Rev 268, 88–103 (2015). [PubMed: 26497515]

56. Roozendaal R, Carroll MC, Complement receptors CD21 and CD35 in humoral immunity. Immunol Rev 219, 157–166 (2007). [PubMed: 17850488]

57. Wernersson S, Kleinau S, Heyman B, Immune complex-mediated enhancement of antibody responses without induction of delayed-type hypersensitivity. Scand J Immunol 52, 563–569 (2000). [PubMed: 11119261]

58. Huber M et al., Complement lysis activity in autologous plasma is associated with lower viral loads during the acute phase of HIV-1 infection. PLoS Med 3, e441 (2006). [PubMed: 17121450]

59. Wei X et al., Antibody neutralization and escape by HIV-1. Nature 422, 307–312 (2003). [PubMed: 12646921]

60. Ackerman ME et al., A robust, high-throughput assay to determine the phagocytic activity of clinical antibody samples. J Immunol Methods 366, 8–19 (2011). [PubMed: 21192942]

61. Gomez-Roman VR et al., A simplified method for the rapid fluorometric assessment of antibody-dependent cell-mediated cytotoxicity. J Immunol Methods 308, 53–67 (2006). [PubMed: 16343526]

62. Brown EP et al., High-throughput, multiplexed IgG subclassing of antigen-specific antibodies from clinical samples. J Immunol Methods 386, 117–123 (2012). [PubMed: 23023091]

63. Almanzar G, Ottensmeier B, Liese J, Prelog M, Assessment of IgG avidity against pertussis toxin and filamentous hemagglutinin via an adapted enzyme-linked immunosorbent assay (ELISA) using ammonium thiocyanate. J Immunol Methods 387, 36–42 (2013). [PubMed: 23022630]

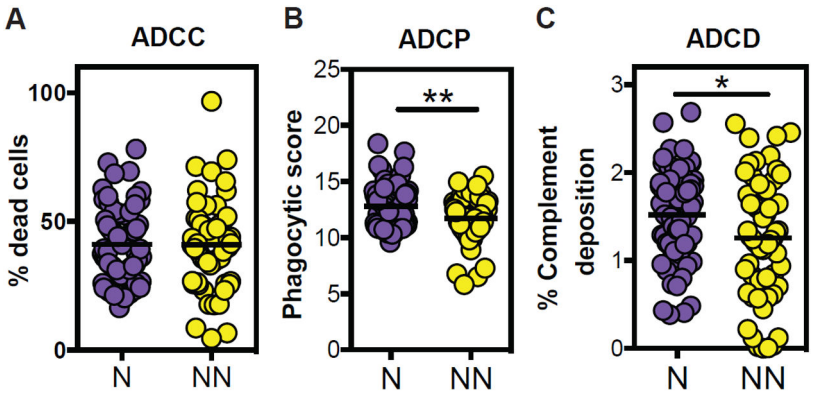

Fig.1:

Unique Fc functional profiling of HIV specific antibodies from Neutralizers. Serum antibodies from Neutralizers (N=purple) and Non-Neutralizers (NN=yellow) were evaluated for their ability to drive NK-dependent ADCC against gp120-pulsed $CD4^+$ cells (A), monocyte directed phagocytosis of gp120-functionalized fluorescent beads (B), or complement deposition (C3b) on the surface of gp120-pulsed $CD4^+$ target cells (C). An unpaired t-test was used for statistical analysis: *p<0.05, **p<0.01.

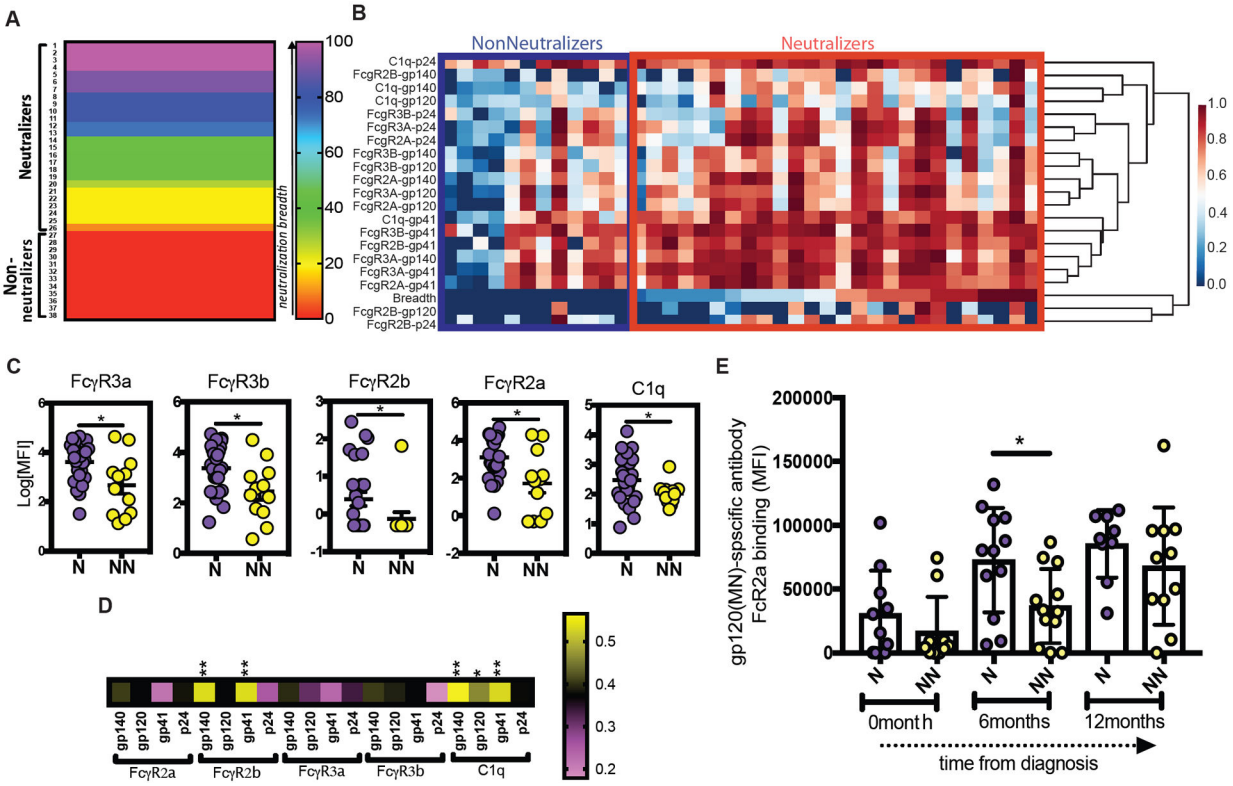

Fig.2:

Enhanced Fc-receptor and complement binding by HIV-specific antibodies in Neutralizers. (A) The heatmap depicts the binding capacity (MFI) of gp140-, gp120-, gp41-, p24-specific serum antibodies to FcγRIIA, FcγRIIB, FcγRIIIA, FcγRIIIB and C1q protein. Each row represents a specific binding except for row 1 where the HIV neutralization breadth is reported. Each column represent one subject, either a Neutralizer (purple) or a non-Neutralizer (yellow). The scale bar represents the Z-normalized scores. (B) The dot plots report the univariate binding of gp120-specific antibodies from each group to FcγRIIA, FcγRIIB, FcγRIIIA, FcγRIIIB and C1q. (C) The dot plot shows the evolution of gp120-specific FcγRIIa binding antibodies in the first year following infection in a group of participants caught in acute HIV infection half of which go on to develop bNAbs (purple) or not (yellow). Each dot represents one subject, with Neutralizers (N) in violet and Non-Neutralizers (NN) in yellow. An unpaired t-test was used for statistical analysis to compare groups, whereas an Anova with a post-hoc Tukey test was used to compare between groups across timepoints. *p<0.05, **p<0.01.

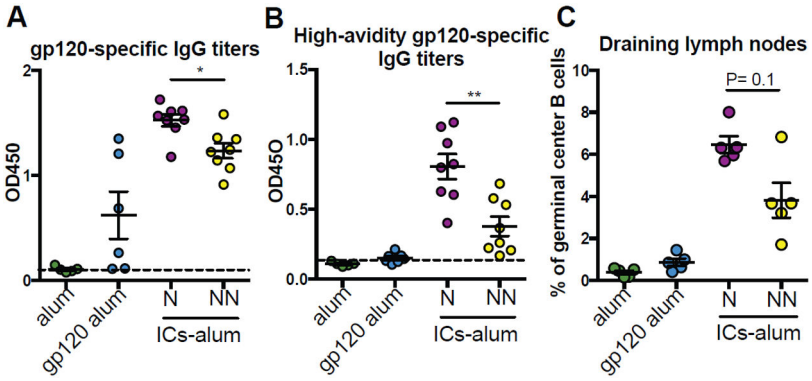

Fig.3.

Neutralizer-immune complexes drive higher avidity antibodies and expanded germinal center B cells. BALB/c mice were immunized twice, 3 weeks apart, with alum-adjuvanted gp120 immune complexes (ICs-alum) generated with serum antibodies from Neutralizers (N) or Non-Neutralizers (NN). Control groups received alum-adjuvanted gp120 or adjuvant alone. Ten days after the last immunization we measured the titers of gp120-specific IgG antibodies (A), the titers of high-avidity gp120-specific IgG antibodies (B) in sera, and the percentage of germinal center B cells (C), defined as live $CD3^{-}CD19^{+}CD38^{-}CD95^{+}$ cells, in draining lymph nodes of immune mice. A two-sided Wilcoxon rank sum test was use to compare responses induced by Neutralizer (N) or Non-Neutralizer (NN) immunized animals. *$p<0.05$

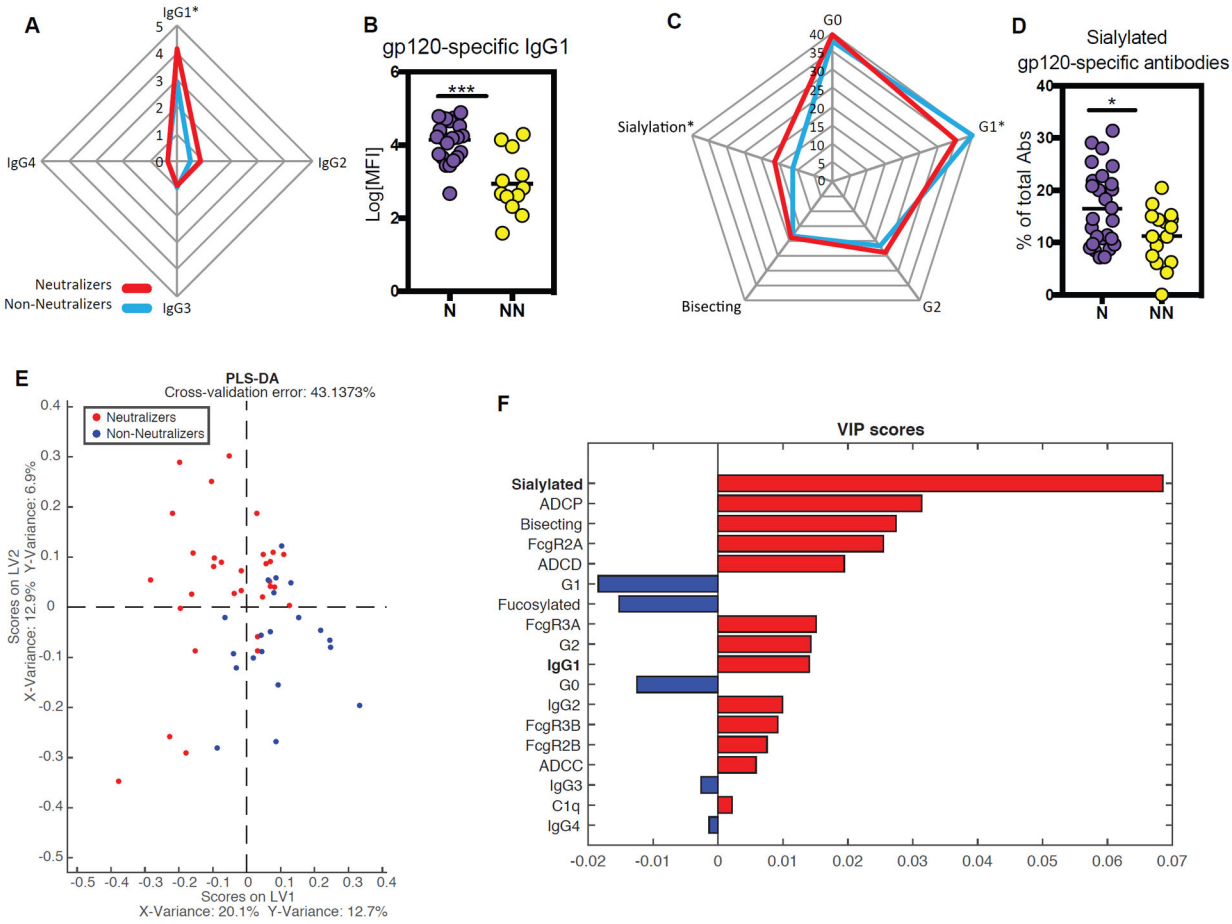

Fig. 4.

Sialylated IgG1 gp120-specific antibodies are increased in Neutralizers. (A) The Radar plot describes the relative differences in gp120-specific IgG1, IgG2, IgG3 and IgG4 antibody titers in sera from Neutralizers (N, red) or Non-Neutralizers (NN, blue). (B) The dot plot shows the gp120-specific IgG1 antibody titer differences. (C) The radar plot describes the relative distribution of gp120-specific IgG antibody glycan levels in sera from Neutralizers (N, red) or Non-Neutralizers (NN, blue). (D) The dot plot depicts the percentage of sialylated gp120-specific IgG antibodies among the groups. An unpaired t-test was used for statistical analysis: *$p<0.05$. (E) The dot plot depicts the PLSDA analysis using all Fc-profile data, including gp120-specific antibody titers, glycan profiles, binding to Fc-receptors and complement proteins, ADCP, ADCD and ADCC, to separate the 2 groups. (F) Variable Importance in Projection (VIP) scores rank the minimal antibody features that are able to separate the Neutralizers (red bars) and non-Neutralizers (blue bar) Fc-profiles.

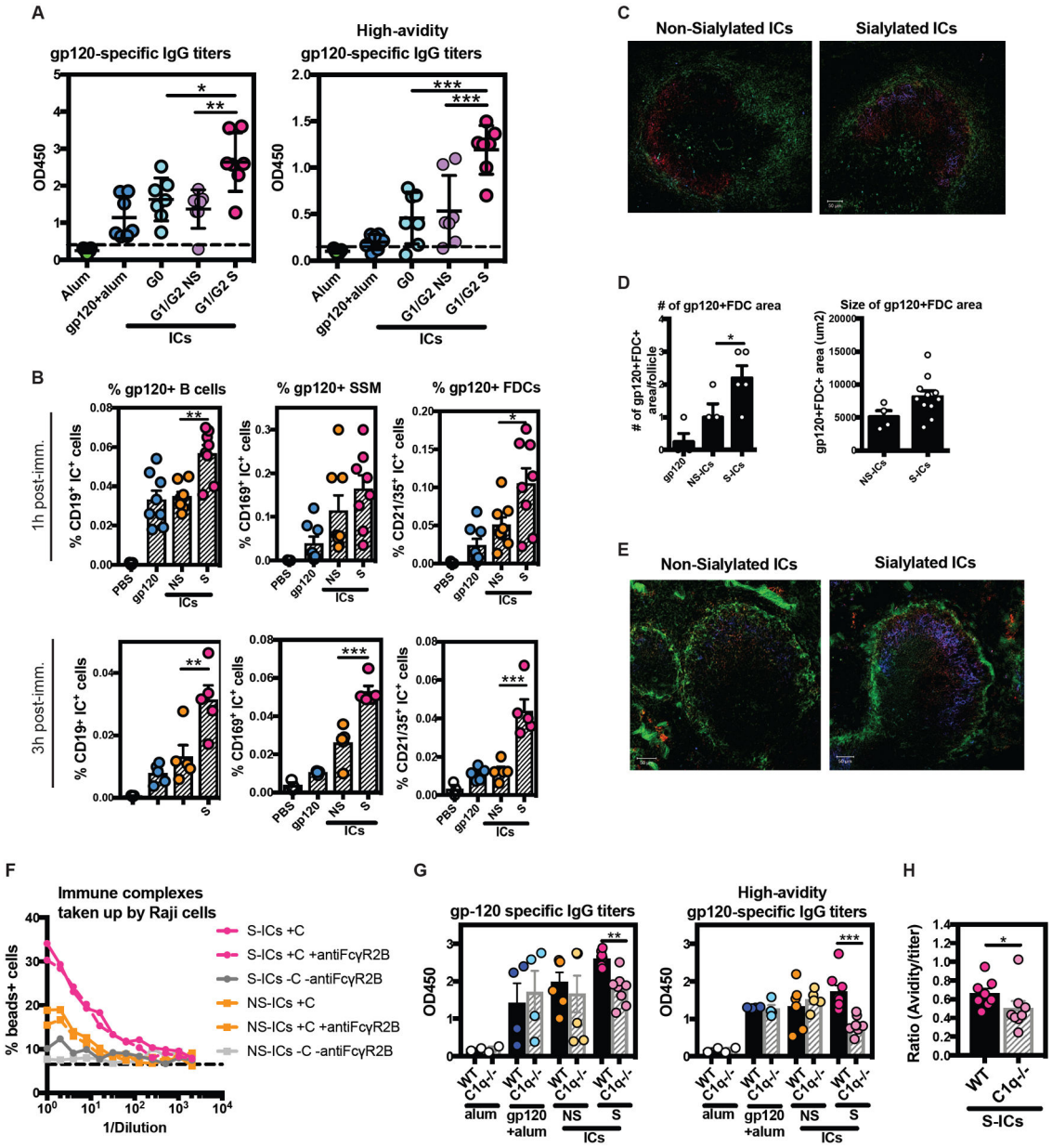

Fig. 5.

Sialylated antibody-immune complexes promote innate and adaptive immunity. (A) The dot plot depicts the antibody titers (left) or avid antibody titers (right) 10 days after the second immunization in Balb/c mice receiving alum alone (green), alum-adjuvanted gp120 (blue), agalactosylated antibodies (G0-Immune Complexes) with alum (aqua), non-sialylated galactosylated antibodies (G1/G2 NS-ICs) with alum (lavender), or sialylated galactosylated antibodies (G1/G2 S-ICs) with alum (pink). (B) The bar graph depicts the number of fluorescently labeled ICs on draining lymphnode non-cognate B cells (gp120+B cells), macrophages (gp120+SSM), or FDCs (gp120+FDCs) after 1h and 3h post injection. (C) The confocal image depicts the level of IC deposition after 1h in a B cell follicle from a mouse immunized with a non-sialylated IC (left) or a sialylated IC (right). (D) The bar graph shows

the number (left) and area occupied (right) of gp120+FDCs in a draining lymphnode. (E) The confocal image depicts IC deposition in a B cell follical 3h after immunization, stained for the antigen (blue), macrophages (green), and GL-7: to detect the germinal center area (red). (F) The line graphs show the role of FcγR2b and complement in glycan-modified IC deposition on a non-cognate B cell, Raji, cells. (G) The dot plot shows the role of complement in the glycan-optimized IC immunization using C57/Black wild type (wt, n=1–4) or C1q−/− knockout (C1q−/−, n=1–4) mice. Both, gp120-specific IgG antibody titers (left) and high-avidity gp120-specific antibody titers (right) are depicted following immunization with alum (white), gp12-alum (blue), non-sialylated galactosylated antibodies (NS-ICs, yellow), or sialylated galactosylated antibodies (S-ICs, pink). One-way ANOVA followed by Tukey's post-test was used for statistical analyses: *$p<0.05$, **$p<0.01$, ***$p<0.001$.